Neutron spectroscopy

Report by
Marcel Brändlein & Jelle Dionot
Group 2

December 4, 2011

Université Pierre et Marie CURIE
Paris VI - Nanomat Master 2

Contents

1 Introduction

Industry is always interested in innovative materials that may bring our present technology a step further. Multiferroics, for example, are fervently discussed at the moment and the number of possible applications is already enormous. It is therefore of major interest to understand the fundamental structure of such materials, that often gives rise to new questions, and it is a physicists task to find the answers. Neutron spectroscopy is the tool of choice and its unique properties can give access to both, the atomic and the magnetic structure of the system. In this report, we will focus on the atomic vibrational structure of calcium fluoride, in order to illustrate the main aspects of inelastic neutron scattering using a triple-axis spectrometer.

2 Basic concepts

2.1 Structure factor

Neutrons are heavy elementary particles, that carry no net charge. Therefore, Coulomb interaction is no longer an issue and the neutrons can interact directly with the nuclei of the crystal atoms of the sample. The differential cross section can give information on the scattering intensity and depends on the Bravais lattice vectors $\vec{R}_n^0$, the transferred momentum $\vec{Q} = \vec{k}_i - \vec{k}_f$ and the energy transfer $\hbar\omega$. It reads

$$\frac{\partial^2\sigma}{\partial\Omega\partial E} = \delta(\omega)\sum_{m,n} e^{i\vec{Q}\cdot\left(\vec{R}_m^0 - \vec{R}_n^0\right)} \left|F(Q)\right|^2 \ , \qquad F(Q) = \sum_l b_l e^{i\vec{Q}\cdot\vec{r}_l} \ , \tag{1}$$

where $F(Q)$ is called the static structure factor and depends on the scattering length b_l and the position $\vec{r}_l$ of atom l in the unit cell. The term with the sum is nothing more than the Bragg condition, or more accurately the Laue equations, which states, that the transferred momentum must be a reciprocal lattice vector $\vec{G}$. In this experiment, we use calcium fluoride, which belongs to the crystal class with highest symmetry, cubic isometric-hexoctahedral, and contains four calcium atoms plus eight fluoride atoms per unit cell. The calcium atoms form a face centred cubic cell with a lattice constant $a = 5.363$ Å and each fluoride atom is positioned in between four calcium atoms to form a tetrahedron. The scattering lengths are given by

$$b_{\mathrm{Ca}} = 0.49 \cdot 10^{-12}\mathrm{cm} \qquad\qquad b_{\mathrm{F}} = 0.56 \cdot 10^{-12}\mathrm{cm} \ .$$

The transferred momentum can be expressed in terms of the Miller indices $\vec{Q} = h\hat{b}_1 + k\hat{b}_2 + l\hat{b}_3$, where $\hat{b}i$ are the reciprocal lattice vectors and are connected to the primitive lattice vectors $\hat{a}_i$. For a cubic system the link is just $\hat{b}_i = (2\pi)/a \ \hat{a}_i$ and in this case the structure factor can be calculated analytically:

$$\begin{aligned} F(h,k,l) = \ & b_{\mathrm{Ca}}\left[\ 1 + e^{-i\pi(h+k)} + e^{-i\pi(k+l)} + e^{-i\pi(l+h)}\right] + \\ & b_{\mathrm{F}}\left[\ e^{-i\frac{\pi}{2}(h+k+l)} + e^{-i\frac{\pi}{2}(3h+k+l)} + e^{-i\frac{\pi}{2}(3h+3k+l)} + e^{-i\frac{\pi}{2}(h+3k+l)} + \right. \\ & \left. e^{-i\frac{\pi}{2}(h+k+3l)} + e^{-i\frac{\pi}{2}(3h+k+3l)} + e^{-i\frac{\pi}{2}(3h+3k+3l)} + e^{-i\frac{\pi}{2}(h+3k+3l)}\right] \end{aligned}$$

We can arrange this equation in a way, that looks more insightful by placing some terms out of the brackets and we finally get

$$F(h,k,l) = \left[1 + e^{-i\pi(h+k)} + e^{-i\pi(k+l)} + e^{-i\pi(l+h)}\right]\left[b_{\mathrm{Ca}} + b_{\mathrm{F}} \cdot e^{i\frac{\pi}{2}(h+k+l)}\left(e^{-i\pi(h+k+l)} + 1\right)\right] \tag{2}$$

The first term in square brackets is the results of the fcc lattice, which gives a first selection rule. It is equal to 4, if h,k and l are all either even or odd. If for example one of them is even, and the other two are odd, then the term would be zero, giving no intensity at all. Looking at the last term in round brackets, this is non zero only if $(h + k + l)$ is even. Therefore, the contribution of the fluorine atoms cancels out for $(h+k+l)$ odd. The exponential term right in front of the round brackets gives a last distinction. It is equal to +1, if $(h+k+l)$ is of the form $2 + 4n$, where n is an integer and -1, if $(h + k + l)$ is of the form $4n$. Putting this all together, we obtain only three different conditions, where Bragg peaks can occur and the structure factor gives

$$\begin{array}{lll} h+k+l \quad \text{even} & \begin{cases} 4n & 4b_{\mathrm{Ca}} + 8b_{\mathrm{F}} \\ 2+4n & 4b_{\mathrm{Ca}} - 8b_{\mathrm{F}} \end{cases} \\ h+k+l \quad \text{odd} & 4b_{\mathrm{Ca}} \end{array} \tag{3}$$

This result will be needed, when aligning the set-up and it means, that only a few $k_{\mathrm{i}} - k_{\mathrm{f}}$ configurations will give intensity.

2.2 Experimental set-up

The set-up used for this experiment is installed on a cold neutron beam line ($T = 20$ K). The energy distribution of the neutrons can thus be express by a Maxwell-Boltzmann distribution

$$f(E)\ dE = \sqrt{\frac{E}{\pi k_{\mathrm{B}} T}} \cdot e^{\left(\frac{-E}{k_{\mathrm{B}} T}\right)}\ dE\ , \tag{4}$$

where k_{B} is the Boltzmann constant. Carrying out the integral for energies from zero to infinity will give an average energy value of the neutrons per degree of freedom, $k_{\mathrm{B}}T/2$. Multiplying this by a factor 3, for the three translational degrees of freedom, we obtain an average energy of $E_{\mathrm{av}} = 2.59$ meV. Using the relation

$$E = \frac{\hbar k^2}{2m_{\mathrm{n}}} \tag{5}$$

according to the wave-particle duality we get a wave vector of $k_{\mathrm{av}} = 1.12\ \mathrm{\AA}^{-1}$. This corresponds to the average size of a Brillouin zone. In our case for CaF_2 the lattice constant of the reciprocal lattice would be $1.172\ \mathrm{\AA}^{-1}$. We see that the energy of cold neutrons is high enough to investigate all the Brillouin zone. However, the low energy limits the window, that we can probe in ω-Q space.

In this experiment we use a basic triple-axis spectrometer. As the name already indicates, this can be divided into three different parts. In a first step a monochromator, based on Bragg's law (angle 1) will chose a certain energy for the incident neutron beam. The monochromator contains several single crystals of the same material, arranged on a spherical plate. This way, the diverging neutron beam will be more focussed after passing the monochromator, leading to a higher intensity. This is needed, because the flux of neutrons decreases rapidly with higher energy, according to the energy distribution. With this method, we are able to get sufficient neutron flux up to about an energy transfer of $E_{\mathrm{i}} - E_{\mathrm{f}} = 15$ meV, where E_{f} is the energy of the scattered neutron beam, to be still chosen. This means, that we are only able to measure acoustic phonons (in phase vibrations) with this set-up, as the optical phonons (out of phase vibrations) are much higher in energy. However, the monochromator does not only give one single energy line, but rather a broadened peak centred around the chosen energy. The linewidth of this peak will set the resolution, that is to say the energy difference at which two different peaks can still

be distinguished. Furthermore, due to higher order Bragg peaks, we will also obtain harmonics ($2\lambda, 3\lambda$ etc.). Although these harmonics will be of lower intensity, they can give rise to spurious signal.
The second part of the set-up contains the sample holder and at this stage, the transferred momentum Q is set. The crystal can be oriented in all three dimensions and according to the structure factor scattering can only occur at a few given orientations towards the incident neutron beam. In this experiment we chose to analyse only the horizontal planes of the crystal, that is to say (h,k,0) planes. There are two possibilities to change Q, either by turning the crystal around a vertical axis (angle 2, variation in k_i) or by varying the angle between incident and scattered beam (angle 3, variation in k_f). In our case we fix k_i and modify only k_f with $k_\mathrm{f} > k_\mathrm{i}$. Thus, according to equation (5) the energy transfer will be negative. We are analysing phonons, and as they are so called quasi particles, they can either be created or annihilated. A negative charge transfer means annihilation of phonons, as the scattered neutron has a higher energy than the incident one. The intrinsic spin of phonons is equal to 1 and Bose-Einstein statistics must be applied,

$$n(E) = \frac{1}{e^{\frac{E}{k_\mathrm{B}T}} - 1} \ . \tag{6}$$

At a given energy this function will rapidly decrease with decreasing temperature. A full treatment based on mechanical statistics will show, that at low temperature, more and more phonons will accumulate in the ground state, giving rise to a Bose-Einstein condensation. These phonons cannot contribute to the dynamical processes any more and thus annihilation is no more possible. This means, that our set-up will become less and less efficient with decreasing temperature. At very low temperature the intensity will be zero.
It remains the energy of the scattered neutrons, which is still to be determined. This is done by the third part, the so called analyser (angle 3). The principle is the same as for the monochromator and a detector sensitive to neutrons will count the scattered neutron for a certain amount of time, that will set the background to signal ratio.
To sum it up, we have four different angles to adjust. The monochromator and analyser (angle 1 and 4) will set the energy transfer, whereas the sampler holder (angle 2 and 3) will set the momentum transfer. Therefore we have in principle access to all points in ω-Q space, however limited by the intensity of the neutrons for a given ω-Q point. In practise one of this parameters will be set to a certain value, and the remaining parameter will be scanned. In this experiment we chose to set the ω fix and vary Q. This will be repeated for different reasonable energy transfers. This way we can resolve the low change in Q when changing ω. The resolution of the so gathered ω-Q map will mainly be determined by the time, available for the measurements.
The whole set-up is driven by a software, which maintains all parameters. Before the measurements can start, the software needs to know the exact orientation of the crystal sample. A first scan is started to find roughly the position of a Bragg 200 peak. If the sample is then turned by 90°, there should also be a peak of the same intensity. If not, that means, the crystal is not in plane. In this case the crystal must be tilted, while holding the 90° constant, until the peak has maximum intensity. After that, the software is calibrated. If we change the geometry, such that we probe the 100 point, it should be zero according to the structure factor (3). However, we were able to still get a signal. Indeed, it was of very low intensity, two orders of magnitude smaller then the 200 peak, but nevertheless distinguishable from the background signal. This might be assigned either to the fact, that the sample cannot be totally monocrystalline, given the size of the sample of several of more than 100 cm^3, or mainly due to the mentioned harmonics. We note also the great quality of the crystal, as the neutrons have to pass through several cm of matter and the scattering length must therefore be of the same order.

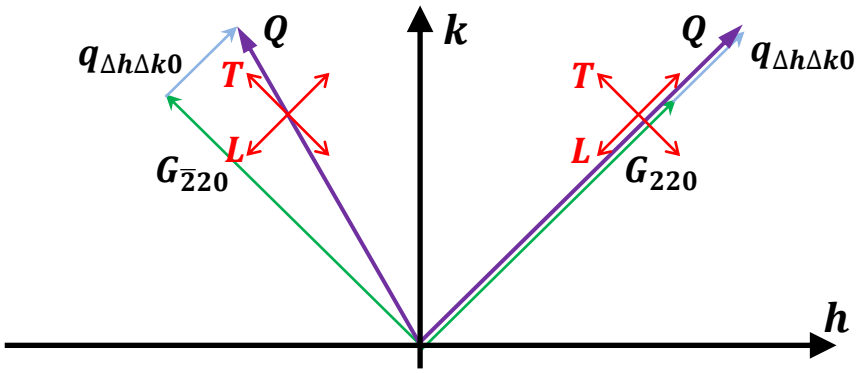

Figure 1: *Schematic sketch of different scattering geometries. In the 220 direction the scanning vector $\vec{q}$ points along the transferred momentum $\vec{Q}$, giving rise to longitudinal phonons. For the $\bar{2}20$ direction the scanning vector will turn $\vec{Q}$, such that both longitudinal and transverse phonons will contribute. The red arrows indicate the displacement vector $\vec{u}_{\mathrm{q}}$.*

2.3 Longitudinal and transverse phonons

Phonons can be divided further into longitudinal and transverse, according to the displacement with respect to the direction of the wave vector. In the presence of phonons, the expression of the cross section in the static case according to equation (1) has to be modified and the cross section for inelastic scattering becomes proportional to

$$\frac{\partial^2\sigma}{\partial\Omega\partial E} \propto \left(\vec{Q}\cdot\vec{u}_{\mathrm{q}}\right)^2 \ , \tag{7}$$

where $\vec{u}_{\mathrm{q}}$ is the displacement vector. Therefore the cross section depends on the angle between the transferred momentum and the displacement vector. This is shown in figure 1 for two different scattering geometries. The transferred momentum is composed of the reciprocal lattice vector $\vec{G}$ plus the scanning vector $\vec{q}$ that will be varied during the measurement. We can see, that for the 220 direction the $\vec{Q}$ vector points in the same direction as the longitudinal displacement vector, but is perpendicular to the transverse one. According to equation (7), only the longitudinal phonons contribute to the signal. For the $\bar{2}20$ direction on the other hand, the $\vec{Q}$ vector is slightly tilted, and the product of $\vec{Q}\cdot\vec{u}_{\mathrm{q,T}}$ is not zero any more. Therefore, both longitudinal and transverse phonons can contribute. However, the scanning vector will be considerably small and the projection of $\vec{Q}$ along $\vec{u}_{\mathrm{q,L}}$ will be very small. Therefore, we will only see the transverse phonons in this configuration. That means, by investigating two identical, but perpendicular Bragg peaks, we obtain either transverse or longitudinal phonons.

3 Results and discussion

Figure 2 shows the experimentally obtained dispersion relation for the acoustic phonons propagating along (hh0). The scans were taken for E = -1 to -15 meV in steps of 1 meV. The monitor was set to 1000, corresponding roughly to 35 s per scan. For higher energy, where the intensity is expected to be lower, the accumulation time has been increased. The two graphs are identically scaled to allow direct comparison. In both graphs we can see a high intensity around (Q,ω)=(0,0), that is rapidly decreasing. For figure 2 (a) the scattering geometry corresponds to the right side of figure 1 and thus shows the longitudinal phonon, whereas 2 (b) corresponds to the left side of figure 1, showing only transverse phonons. According to theory, there are two transverse phonons and one longitudinal phonon. However, the transverse phonons are to close

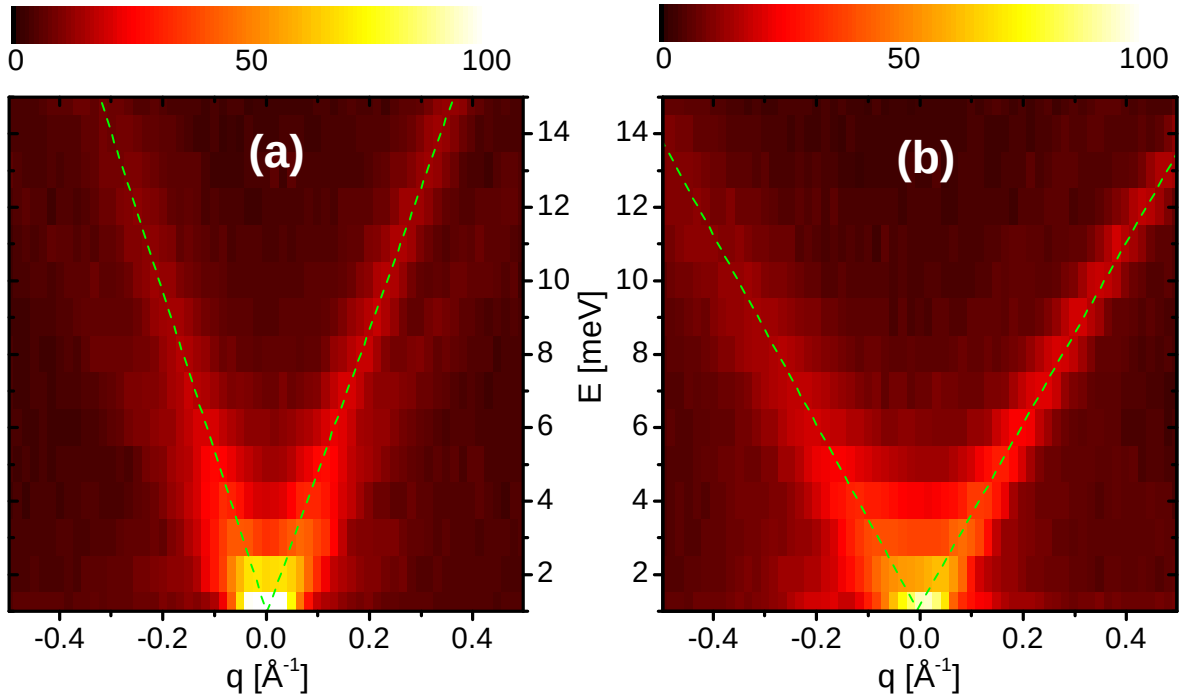

Figure 2: *Dispersion relation of CaF_2 for two different reciprocal lattice vectors G_{220} (a) and $G_{\bar{2}20}$ (b). (a) corresponds to longitudinal phonons and (b) to transverse phonons. In order to get better contrast, the square root of the intensity is taken. The dashed lines indicate a linear fit. Additionally we can see a second branch in (a), with lower slope. However, the fit is not shown, because it would hide the data.*

and cannot be resolved by this technique. By extracting the position of the peaks for each scan we are able to fit the dispersion curve. As we only probe a small region of the brillouin zone with $q = (hh0) \cdot 2\pi/a$, the expected dispersion relation in the limit of long wavelengths should be linear and indeed we find a linear relation. With an adjusted R-square between 0.998 and 0.998 the fits show almost perfect agreement with the data. The peaks for each scan are extracted by multiple peak fitting using a pseudo-Voigt function.
Given the slope of the curves we can calculate the sound velocity of the phonons. The group velocity of a propagating wave is given by the derivative of ω with respect to the wavevector

$$v_g = \frac{\partial \omega}{\partial q} = \frac{1}{\hbar}\frac{\partial E}{\partial q} \tag{8}$$

The following table shows the slopes and the calculated group velocities for (a) and (b):

(a)		(b)	
slope $\left[meV^{-1}\right]$	$v_g\left[10^3\frac{m}{s}\right]$	slope $\left[meV^{-1}\right]$	$v_g\left[10^3\frac{m}{s}\right]$
50.891	6.599		
-45.434	5.892		
27.739	3.597	30.285	3.927
-27.541	3.571	-29.002	3.761

As expected, the slope for transverse phonons is lower than the one for longitudinal phonons and accordingly transverse phonons propagate slower than longitudinal phonons. Surprisingly, we can see an additional branch in (a), for which only longitudinal phonons should occur. It is very

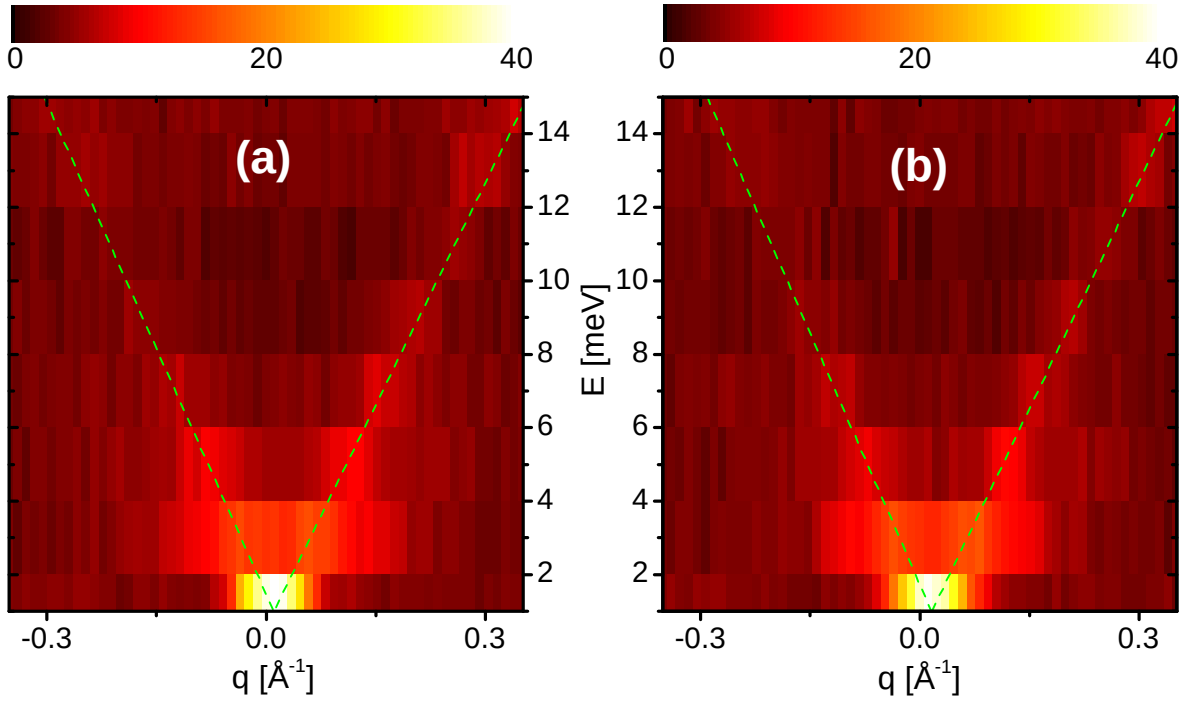

Figure 3: *Dispersion relation of CaF_2, similar to figure 2, but for G_{200} (a) and $G_{\bar{2}00}$ (b). The dashed lines indicate again a linear fit. Only half as much scans per graph were taken, resulting in a less resolved map. The slopes in graph (a) and (b) are almost identical. Furthermore, the overall intensity less, compared to figure 2.*

weak in intensity, and only about 3 to 5 points could be extracted from the scans. Reasonable values for the slope and therefore the group velocity could only be obtain by taking additionally the value of the single peak at 1 meV. The values correspond, to the ones obtained for transverse phonons in (b), giving rise to the assumption that we can see not only longitudinal phonons in (a) as expected, but also transverse ones. This might be due to harmonics or to a wrongly oriented crystal.

We can see a bigger difference for the two values for negative and positive slopes for the longitudinal phonon probed in (a). This might be due to the fact, that an additional branch occurs, that disturbs the peaks of the longitudinal phonon scans at low energy, giving rise to slightly shifted values. Nevertheless, the obtained values look reasonable and are of the order of magnitude of other solid materials (quartz glass $v_g = 5.37\ 10^3$m/s).

The same measurements were also taken for phonons propagating along the (h00) direction. This is shown in figure 3. We can see the same aspects, however less resolved, due to a limited amount of time. The scans are now taken from E = -1 to -15 meV in steps of 2 meV. This time no additional branch can be seen in graph (a). Furthermore, the slopes obtained by linear fitting are almost identical for both graphs, as the following table will show:

(a)		(b)	
slope $\left[meV^{-1}\right]$	$v_g\left[10^3\frac{m}{s}\right]$	slope $\left[meV^{-1}\right]$	$v_g\left[10^3\frac{m}{s}\right]$
52.247	6.775	53.505	6.938
-47.813	6.131	48.403	6.277

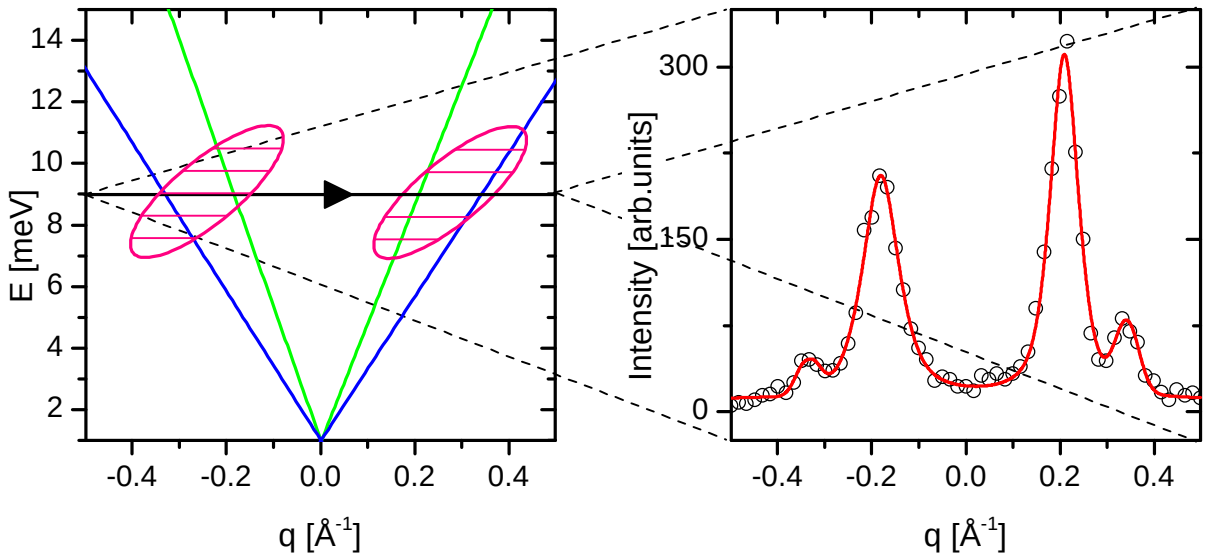

Figure 4: *Illustration of the defocussing effect. Due to the instrumental resolution the probed ω-Q point will become a tilted ellipse. This leads to a different accumulation for the different overlap.*

Compared to DFT calculations[1] it becomes clear, why we cannot see the transverse phonons. The (h00) direction points towards the X point in the brillouin zone and the slope of the transverse phonons very low and thus these branches lie outside the detected window. However, it is again not clear, why we should obtain almost the same group velocity for both graphs. This can either mean, that the transverse phonons have an almost identical dispersion relation than the longitudinal ones for this given direction. Another possible explanation is again, that the initial calibration of the set-up was not done properly and therefore the scanning vector might not be totally aligned with $\vec{Q}$ for (a) (or be perpendicular for (b)), leading to a contribution of both transverse and longitudinal phonons. However, we note that the group velocity is similar than the one obtained in figure 2. This seems reasonable, as the dispersion relation for longitudinal phonons in the limit of long wavelengths does not change much for different scanning directions. Furthermore, we can see that the intensity range is reduced by a factor of about 2.5. If we look at the intensities using the structure factor for the two different scanning directions according to equation 3, the ratio becomes

$$\left|\frac{F(2,2,0)}{F(2,0,0)}\right|^2 = \left|\frac{6.44\ 10^{-12}\text{cm}}{-2.52\ 10^{-12}\text{cm}}\right|^2 = 2.56^2$$

In figure 2 and 3 the square root of the intensities are taken, and thus the different intensities can be explained by the structure factor alone.

If we take a closer look at a single scan, we can furthermore see, that the peaks for positive and negative q are not of the same intensity. This is an artefact of the experimental set-up and is shown in figure 4 for an energy of 9 meV and a scanning direction along (hh0). With a perfect set-up, we would probe a given ω-Q point with a δ-function. However, this is far from the real world. The finite resolution of the spectrometer gives rise to a resolution function. A convolution between the resolution function and the delta function will give a Gaussian function. As indicated in figure 4 the ω-Q spot will rather be a tilted ellipsoid. We can directly see, that the

[1] K. Schmalzl, D. Strauch, H. Schober, Phys. Rev. B 68, 144301 (2003)

overlap between ellipsoid and the dispersion relation is less for negative q compared to positive q. Hence, the intensities will be different.

4 Conclusion

We have seen, that neutrons are perfect probes, when we want to investigate the dispersion relation of phonons. A typical neutron source will allow to vary the neutron energy over a great range, giving thus access to different branches in phase space. A triple-axis set-up can be made sensitive to either transverse or longitudinal phonons, according to the orientation of the scanning vector with respect to the reciprocal lattice vectors. The main drawback is the time needed to accumulate enough signal, in order to be able to distinguish signal from noise and this will set the resolution of the obtained phase space maps. We were able to obtain the dispersion relation for calcium fluoride along two different high symmetry directions, in the limit of long wavelengths. From that, we could derive the sound velocity of both longitudinal and transverse phonons. We conclude, that neutron spectroscopy is a powerful and accurate technique, that reveals the vibrational structure of solid matter. Furthermore, it can give information also on the magnetic structure, that unfortunately could not be treated within this experiment. But there is still time to get into that as well.